© 2018 IJSRSET | Volume 4 | Issue 1 | Print ISSN: 2395-1990 | Online ISSN : 2394-4099
Themed Section : Engineering and Technology

Synthesis, Characterization and Antimicrobial Activity of Sulphur doped ZnO Nanoparticals

A. E. Athare
Department of Chemistry, New Arts, Commerce and Science College , Ahmednagar, Maharashtra, India

ABSTRACT

Sulfur-doped Zinc Oxide (ZnO) nanowires were successfully Synthesized by C0-precipitation method. The structure morphology chemical composition and antibacterial activity as synthesized S-doped ZnO nanostructures were investigated. X-ray diffraction and the selected area electron diffraction results reveal that the synthesized products are single-phase with hexagonal wurtzite structure with a highly preferential orientation in the (101) direction. EDS-shows that the above route produced highly pure S-doped ZnO nanostructures. The optical band gaps of various ZnO powders were calculated from UV-Visible diffuse reflectance Spectroscopic studies. The FTIR spectrum shows that S-doping had an obvious effect on the stretching and bending frequency.

Keywords: Nanoparticles, XRD, SEM, Antibacterial activity.

I. INTRODUCTION

Zinc oxide (ZnO) is a wide band gap (3.37ev), II-VI semiconductor of great interest for optoelectronic applications. [1-3]. It's advantages over other wide band gap materials include eco-friendliness, resistance to oxidation, low cast, and a large excitation binding energy [60mev] (4).

In ZnO has well-documented emission bands of varying strengths the band edge ultraviolet (UV) emission and a broad defect mediated green emission [1-3]. Variously shaped ZnO nanoparticles are routinely synthesized and their electrical and optical properties have been exploited for many exciting applications including nanolasers, phosphors, light emitting diodes, biosensors, solar cell, and electrical generators [1, 5-09].

Mg and transition metals in ZnO has been carried out in order to obtain novel properties and broadens possible applications [11-14]. However, little attention has been paid to S doping in ZnO because of the difference between the low stability of sulfur and the high growth temperature of ZnO. Sulfur has a much smaller electro negativity (2.58) than that of oxygen (3.44) and the atom radius of Sulfur (1.09 A^0) is much larger than that of oxygen (0.65A^0). The difference between S &O makes it possible to obtain some novel properties of ZnO via S doping. Yoo et al. have reported that the band gap of ZnO could be tuned via S dopant [15]. Impurities are also expected to increase the electrical conductivity of ZnO by supplying excess carriers [16].

ZnO nanostructures offer new and enhanced properties that differ from the bulk powder due to their high surface to volume ratio [1, 13]. The synthesis of hexagonal shaped ZnO nanostructures by surface doping hexagonal ZnO nanowires with thiourea (NH_2CSNH_2) in a low temperature solution based process. Scanning electron microscopy (SEM) reveals that the cross sectional shape of the nanostructure strongly depends on sulfur doping levels. Energy dispersive X-ray spectroscopy (EDX)

confirms that the synthesis process yields pure ZnO nanoparticls. UV-Visible absorption spectroscopy is a band gap semiconductor with an energy gap. The antibacterial activity of ZnO nanoparticles is systematically tested against gram positive and bacteria and gram negative bacteria by using agar well method. FTIR shows ZnO doped sulphur stretching and binding frequency.

II. METHODS AND MATERIAL

Zinc Sulphate [$Zn(SO_4).7H_2O$], Thiourea (NH_2CSNH_2) and poly ethylene glycol (PEG-500) were used in the experiment. The ammonia (NH_3) as a precipitating agent and deionised water is used for the preparation of solutions. The $Zn(SO_4).7H_2O$, Thiourea (NH_2CSNH_2) and polyethylene glycol (PEG-500) are mixed together and grinding using an agate mortar. Then this mixture was dissolved in 300 ml deionised water. The solution was dispersed in ultrasonic bath and to this solution excess of ammonia was added to get precipitate. Then the solution was refluxed for 4 to 5 hours and white precipitate was isolated by filtration, washed with deionised water and ethanol. Then dried in a vacuum oven at 60 ^{0}c for 24 hours to obtain powder form. Finally Sulphur doped ZnO nanoparticles were obtained after annealing of the precursor in air at 500^{0}C for two hours respectively.

III. RESULTS AND DISCUSSION

The prepared samples were characterized by various sophisticated Techniques. The X-ray analysis (XRD) of samples is obtained using Philips X-ray diffractometer with diffraction angle 2θ in between 20 to 80° using Cu-Kα radiation of wavelength 1·54058 Å. Surface morphology and elemental analysis of the samples were carried out using scanning electron microscopy with electron dispersion spectroscopy (SEM-EDS) characterization conducted using a JEOL-JED 2300 (LA) instrument. The FT-IR study was done in the range of 4000-500 cm^{-1} by JASCO-FTIR/4100spectrometer with anhydrous KBr as standard reference. The light absorption by sample was carried out by using Varian Carry 5000 (UV-VIS-DRS) spectroscopy in the range 800-300 nm.

Figure 1 Shows that the S-doped ZnO nanoparticles are XRD peaks significantly broader as compared to bulk samples [17]. Briefly, a peak in the diffracted intensities has been shows formation of nanoparticles in the crystal [18].

XRD pattern of the sample has prominent peaks at two theta values of 31.73^0, 34.37^0, 36.21^0, 47.470, 56.55^0, 62.77^0, corresponding to (100), (002), (101), (102), (110), (103). The lattice constants of our sample are found to be a = b = 3.242 A^0 and c = 5.176A^0 in good agreement with the values of hexagonal ZnO. The (hkl) values are also in good agreement with the standard card of ZnO powder [19].

The particle size was calculated by Debye-Scherer's equation using most intense peak (101)

$$D = \frac{k\lambda}{\beta \cos\theta}$$

Where D is the crystallite size, K is a constant (shape factor about 0.9) λ is the x-ray wavelength (1.5405 nm), β is the full width at half maximum (FWHM) of the diffraction line and Θ is the diffraction angle. Average particle size was found to be 09.11 nm.

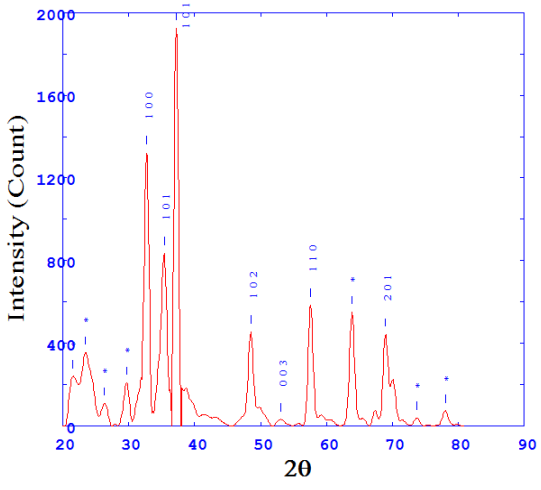

Figure 1. XRD Pattern of S-doped ZnO calcined at 500°C.

FT–IR spectra of S-doped ZnO samples in the range of 4000 to 500 cm^{-1}. Fig.(2) shows that the spectra shows a broad absorption peak around 3311 cm^{-1} and a sharp peak around 1600 cm^{-1}, which represents the surface adsorbed water and hydroxyl groups. In addition, a weak absorption peak around 3693 cm^{-1} was observed , may be due to the tetrahedral coordinated vacancies (Zn^{2+}–OH) , a broad peak around 630 cm^{-1} was also observed, may be due to the Zn–O stretching and Zn–O–S bending, characteristic of the anabas structure of S-doped ZnO. No absorption peaks corresponding to samarium were observed, results are in good agreement with XRD.

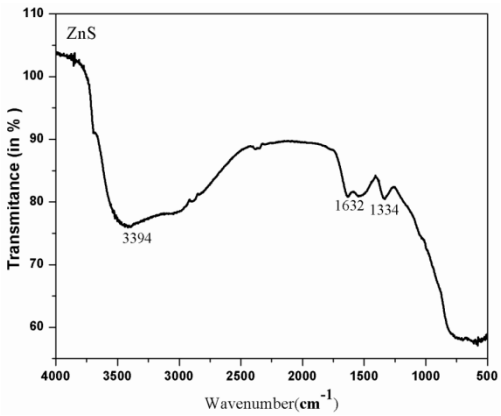

Figure 2. FT-IR spectra of S-doped ZnO calcined at 500°C.

The SEM image of ZnO nanoparticle is shown in figure 3 a high degree of agglomeration is clearly visible in agreement with previous studies [20]. The observation of some larger nanoparticles in SEM image is attributed to agglomeration [21]. In EDX spectrum of ZnO nanoparticles, a sample is shown in fig (3). The names and percentages of the elements further ZnO sample are shown in the labelling clearly, Zn and O are the main constituents of the sample [22] and no trace of impurities could be found within the detection limit of EDX.

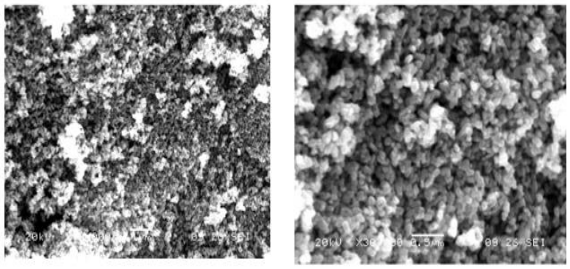

Figure 3. SEM images of S-doped ZnO nano particles calcined at 500 °C with PEG as asurface directing agent.

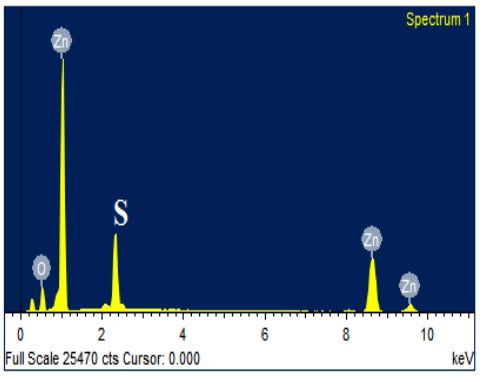

Figure 4. EDX Pattern of S-doped ZnO nanoparticles.

The band gap energies (Ebg) of the S-doped ZnO nanoparticles were probed by UV-Visible diffusion reflectance spectroscopy (UV- DRS). It determine band gap of the prepared materials. Figure 4 shows that The diffusion reflectance spectra were recorded and cut off wave length at which absorption sharp edge rises were determined by drawing a tangent on this curves (402.7). The band gap energies were calculated by using cut off wavelength is represented in the following table. The band gap energy is calculated by using the hollowing equation Ebg =1,240/λ. Where **λ is** the wavelength in nanometer and Ebg is the band gap energy of synthesized nanomaterial was found to be 3.07 ev.

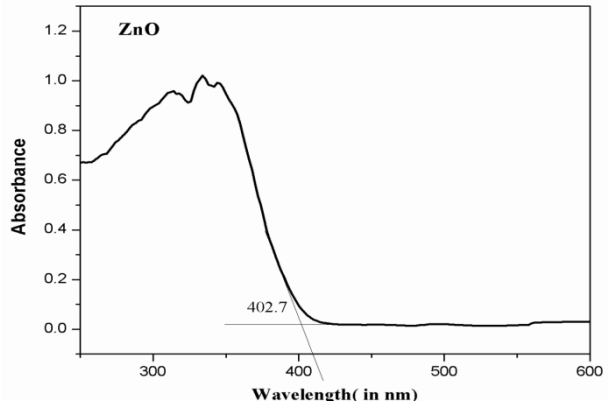

Figure 5. DRS image of S-doped ZnO nanoparticles.

The antimicrobial test of ZnO nano particles was taken against various micro-organism such as S. aureus, B. cereus, E. coli, P. aeruginosa. Anti-microbial activity was determined by Agar Cup Diffusion Method. The S-doped ZnO nanoparticle were dissolved in DMSO i.e.-di-methyl sulphoxide and ultrasonicate.

Figure 5. Antimicrobial activity.

Table 1

Sr. No.	Test microorganisms	Sample I Zone of inhibition in'mm'	
		50µg/ml	100µg/ml
1	S. aureus	-	-
2	B. cereus	-	-
3	E. coli	-	-
4	P. aeruginosa	**09**	**09**
5	Negative control	-	-

IV. CONCLUSION

Sulfur doped ZnO nanoparticles were prepared by a simple, fast and low cost co-precipitation method. The synthesis of Sulphur doped ZnO nanostructures (spherical morphology) EDX shows the elemental composition of synthesized nanoparticles. Synthesized nanoparticles show 3.07 ev band gap energy which slightly lower than commercial ZnO doped sulfur (3.17 ev). The absorption spectra due to Zn-O stretching were observed at 3394 cm^{-1}, 1632 cm^{-1}, 1334 cm^{-1}, the synthesized nanoparticles shows excellent biological activity for P. aeruginosa.

V. REFERENCES

[1]. U. Abulimen, mater. Res. SOC. Symp.Proc., 1, 27.1 (2005)

[2]. Foreman, J.V.; LI, V.; Peng, H.; Chol, S.; Everltt, H. O.; Ltu, J. Time-resolved in vestigation of bright visible wavelength luminescence from Sulfur-doped ZnO nanowires and micropowders. Nano Lett. 2006, 6, 1126-1130.

[3]. Djurisic, A. B.; Leung, Y. H. optical properties of ZnO nanostructures. Small 2006, 2, 944-961. DOI:10.1002/smll.200600134.

[4]. Foreman, J. V.; Everitt, H. O.; Yang, J.; Liu, J. Influence of temperature and photoexcitation density on the quantum efficiency of defect emission in ZnO powders. Appl. Phys. Lett. 2007, 91,011902. DOI: 10.1002/smll.200600134.

[5]. Ozgur, U.; Alivov, Y. I.; Liu, C.; Take, A,; Reshchikov, M. A.; Dogan, S.; Avrutin, V.; Cho, S. J.; Morkoc, H. A Comrehensive review of ZnO materials and devices. J. Appl. Phys. 2005, 98, 041301.DOI: 10.1063/1.1992666.

[6]. Zhang, X. M.; Lu, M. Y.; Zhang, Y.; Chen, L.J.; Wang, Z. L. Fabrication of a high-brightness blue-light-emitting diode using a ZnO nanowire array grown on P-GaN thin film. Adv. Mater. 2009, 21, 2767-2770. DOI: 10.1002/adma.200802686.

[7]. Yeh, P. H.; Li, Z.; Wang, Z. L. Schottky-gated probe-free ZnO nanowirre biosensor. Adv. Mater. 2009, 21, 4975-4978.

[8]. Weintraub, B.; Wei, Y.; Wang, Z. L. Optical fiber/nanowire hybrid structures for efficient three-dimensional dye-sensitized solar cells. Angew. Chem. Int. Edit. 2009, 48, 8981-8985. DOI: 10.1002/anie.200904492.

[9]. Wang, Z. L.; Song, J. Piezoelectric nanogenrators based on zinc oxide nanowire arrays. Science 2006, 312, 242-246. DOI: 10.1126/science.1124005.

[10]. Wang, X.; Song, J.; Liu, J.; Wang, Z. L. Direct-Current nanogenerator driven by ultrasonic waves. Science 2007, 316, 102-105. DOI: 10.1126/science.1139366.

[11]. Xu, S,Qin, Y.; Xu, C.; Wei, Y.; Yang, R.; Wang, Z. L. Self-powered nanowire devices. Nat. Nanotechnol. 2010, 5, 366-373. DOI:10.1038/nnano.2010.46.

[12]. Y. Z. Yoo, T. Fukumara, Z. Jin, K. Hasegana, M. Kawasaki, P. Ahmet, T. Chikyow and H. Koinuma, J. Appl. Phys. 90, 4246 (2001) DOI: 10.1063/1.1402142.

[13]. A. Ontomo, M. Kawasaki, T. Koida, K. Masubuchi, H. Koinuma, Y. Sakurai, Y. Yoshita, T. Yasuda, and Y. Segawa, Appl. Phys. Lett. 72, 2466 (1998). DOI: 10.1063/1.124573.

[14]. S. Choopun, R. P. VIspute, W. Yang, R. P. Sharma, T. Venkatesan and H. Shen, Appl. Phys. Lett., 80, 1529 (2002). DOI: 10.1063/1.1456266

[15]. Y. Z. Yoo, Y. Osaka, T. Fukumura, Z. W. Jin, M. Kawasaki, H. Koinuma, T. Chikyow, P. Ahmet, A. Setoguchi, and S. F. Chichibu, Appl. Phys. Lett., 78, 616 (2001). DOI: 10.1063/1.1344572

[16]. Y. Z. Yoo, Z. W. Jin, T. Chikyow, T. Fukumura, M. Kawasaki and H. Koinuma, Appl. Phys. Lett., 81, 3798 (2002). DOI: 10.1063/1.1521577

[17]. S. Kawano, J. Takahashi and S. Shimada, J. Am. Ceram. Soc. 86, 701, (2003). DOI: 10.1111/j.1151-2916.2003.tb03360.x

[18]. Jian MZ,Yan Z, Ke-Wei X, Vincent J.General compliance transformation relation and applications for anisotropic hexagonal metals. Solid State Communications 2006; 139: 87-91.DOI: 10.1016/j.ssc.2006.05.026.

[19]. Tamus U. The Meaning of Size Obtained from Broadened X-ray Diffraction Peaks. Advanced Engineering Materials 2003; 5:323-329.

[20]. Powder Diffraction File, Alphabetical Index, Inorganic compounds, Published by JCPDS International Center for Diffraction Data, Newtown Square, PA.19073,2003;5:323-329.

[21]. Chou TP,Qifeng Z, Glen EF, Guozhong C. Hierachically Structured ZnO Film for Dye-Sensitized Solar Cells with Enhanced Energy Conversion Efficiency. Adv Mater 2007; 19;2588-2592. DOI: 10.1002/adma.200602927

[22]. Caglara M, Yakuphanoglub F. Structural and Optical properties of copper doped ZnO films derived by Sol-gel. Applied Surface Science 2012;258: 3039-3044. doi: 10.4172/2165-8064.1000328